Journal of Alloys and Compounds 509 (2011) 4495–4498

Contents lists available at ScienceDirect

Journal of Alloys and Compounds

journal homepage: www.elsevier.com/locate/jallcom

Martensitic transformation of Ti50Ni30Cu20 alloy prepared by powder metallurgy

M. Valeanu[a,*], M. Lucaci[b], A.D. Crisan[a], M. Sofronie[a], L. Leonat[b], V. Kuncser[a]

[a] National Institute of Materials Physics, 077125 Bucharest, Romania
[b] National Institute for Electrical Engineering ICPE-CA, 030138 Bucharest, Romania

ARTICLE INFO

Article history:
Received 10 December 2010
Received in revised form 17 January 2011
Accepted 20 January 2011
Available online 2 February 2011

Keywords:
Ti–Ni–Cu shape memory alloy
Powder metallurgy
Martensite transformation
Phase content
Metals and alloys
Powder metallurgy
Shape memory
Calorimetry
X-ray diffraction

ABSTRACT

Phase transformation behavior of Ti50Ni30Cu20 shape memory alloys prepared by powder metallurgy is analyzed with respect to the duration of mechanical alloying. The processed blends were studied by differential scanning calorimetry and room temperature X-ray diffraction. The martensitic transformations evidenced by thermal scans are discussed in correlation with the relative phase content obtained from the refinement of the X-ray diffraction patterns.

1. Introduction

It is known that the near equi-atomic Ni–Ti shape memory alloy (SMA) undergoes a thermo-elastic reversible structural transformation between the high temperature austenite phase with cubic structure (B2) and the low temperature martensite phase with monoclinic structure (B19′). Function on the metallurgical and mechanical conditions as well as the chemical composition, the transformation may take place either in one-stage (B2–B19′) or in two-stages, in the last case, via an intermediate phase with rhombohedral symmetry (*R*). The large lattice distortion, responsible for the important shape memory effect (SME) in Ni–Ti alloys is accompanied by a broad thermal hysteresis which prolongs the functional response. This inconvenience seems to be surpassed in ternary alloys by the partial substitution of one of the alloy's elements. Replacing a part of nickel atoms by copper, the transformation behavior is changed, bringing a lot of advantages in practical use. It was reported that copper substitution narrows the transformation hysteresis, improves the transformational cyclic behavior and reduces the sensitivity of characteristic transformation temperatures to the alloy composition [1,2]. In addition Ti–Ni–Cu alloys, with Cu concentration between 7.5 and 15%at show a two-stage transformation, B2–B19 (orthorhombic structure)–B19′, while for Cu content higher than 15% the second transformation (B19–B19′) may be either suppressed or pushed down to lower temperatures [1,3]. Although the SME of B2–B19 transformation is smaller than that of B2–B19′ transformation, the faster response due to the narrow transformation hysteresis, makes Ti50Ni50–*x*Cu*x* (with $15 > x > 25$) a very attractive actuator material.

Conventionally, these alloys are prepared by melting techniques, in arc or induction furnace, followed by specific thermo-mechanical treatments for homogenization and aging and additional mechanical machining to get the needed shape. All these processes are done under vacuum or inert atmosphere because oxidation damages drastically the properties. Recently there has been significant interest in adopting new non-conventional techniques such as powder metallurgy (PM) based on a high-energy ball-milling process [4] or rapid solidification [5] for manufacturing the NiTi based alloys, especially those with Cu content higher than 15% which are brittle and the plastic working is not easy to be done. It is worth to mention that the shape recovery performances evaluated by tensile strain versus temperature on NiTi or NiTiCu alloys prepared by PM are only little diminished compared with whose prepared be classical melting route [6]. However by these

* Corresponding author at: National Institute of Materials Physics, Magnetism Laboratory, Atomistilor Str. 105 bis, 077125 Magurele, Bucharest, Ilfov, Romania. Tel.: +40 21 3690170; fax: +40 21 3690177.
E-mail addresses: valeanu@infim.ro, mihaela@donnamaria.ro (M. Valeanu).

0925-8388/$ – see front matter © 2011 Elsevier B.V. All rights reserved.
doi:10.1016/j.jallcom.2011.01.154

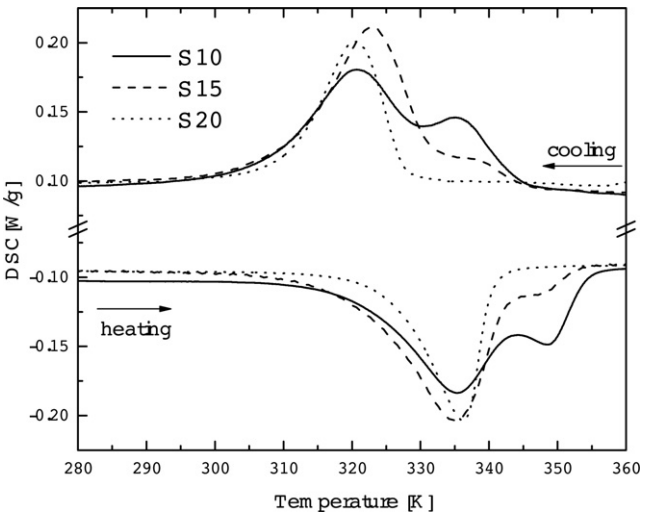

Fig. 1. DSC curves of Ti50Ni30Cu20 alloys mechanical milled 10 (S10), 15 (S15) and 20 (S20) hours.

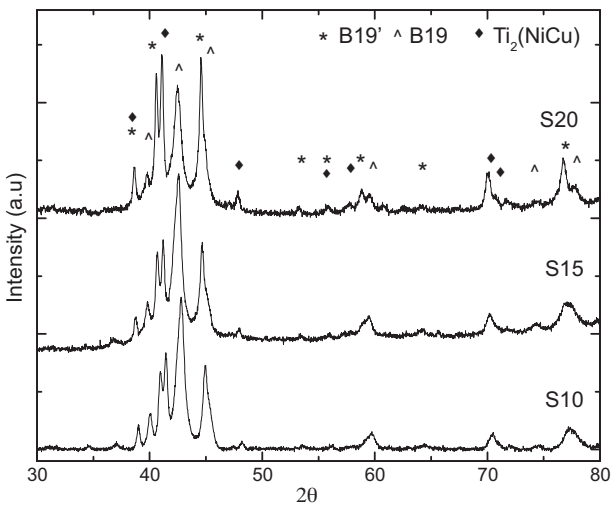

Fig. 2. Room temperature X-ray diffraction patterns of Ti50Ni30Cu20 alloys prepared after different milling time.

non-conventional methods the classical thermo-mechanical treatments can be avoided and ribbons or pieces of complex shape may be directly obtained, besides low-cost and a good composition control. On the other hand, powder processing includes easy oxidation and high porosity of the final products. In this regard, in the last years there are studies concerning the influence of sintering temperature and time [7], and of the rotating speed during ball milling [4,8], on the alloys homogeneity and porosity. In addition to the mentioned results, this study reports on the influence of mechanical milling time on phase transformation behavior of Ti50Ni30Cu20 prepared by PM.

2. Experimental procedures

Metallic powders with over 99.95% purity were weighed stoichiometrically to obtain the Ti50Ni30Cu20 (at %) system. The elemental powders were mechanical milled for 10 (sample S10), 15 (sample S15) and 20 (sample S20) hours respectively, in petroleum ether media. The ball/powder ratio was of 5:1 and the revolution speed was of 350 rpm. The as-milled powders were compacted by uni-axial cold pressing with 400 MPa and then sintered at 950 °C in argon atmosphere for 1 h. Finally, on all the samples was applied an aging treatment at 450C for 4 h.

The samples were investigated by X-ray diffraction using a D-8 Advance Bruker diffractometer with Cu Ka radiation. The phase transformation temperatures were determinate by differential scanning calorimetry (DSC) via a Netsch Differential Scanning Calorimeter – model 204 F1 Phoenix under a scanning rate of 10 K/min. Two samples have been also examined by transmission electron microscopy (TEM) using a JEOL 200CX microscope operating at 200 kV. The TEM specimens have been prepared by mechanical polishing followed by ion milling on a Gatan Duo Mill installation.

3. Results and discussions

3.1. Martensitic transformation

The thermal scans presented in Fig. 1 prove of the martensitic transformation in the prepared specimens (S10, S15 and S20). The transformation temperatures determined by the tangential line method as well as the heat of transformation calculated using the Netsch software, are presented in Table 1. In the case of samples mechanical milled for 10 and 15 h, S10 and S15, two peaks are observed. They may be attributed to two independent transformations or to a two-step transformation. By increasing the milling time the first transformation peak (by cooling) is diminishing so that for alloy S20 only one transformation, proved by one sharp peak, is evidenced. The thermal hysteresis, i.e. the difference between austenite finish (Af) and martensite start (Ms) temperatures is no higher than 12 K; such a narrow thermal hysteresis is characteristic for copper substituted NiTi alloys and is generally associated with martensitic transformation toward orthorhombic type structure. The range of martensitic transformation (Af–Mf) is rather wide (>30 K) like in the cubic to monoclinic transformation.

These data are strange and in disaccord with the expected results. For an alloy with the same composition (Ti50Ni30Cu20) but prepared by casting method, it is reported [1] only one transformation in the ambient temperature range, from the cubic austenite to orthorhombic martensite; the second transformation, from orthorhombic martensite to monoclinic one (B19–B19′), is pushed down to lower temperatures (<150 K) and due to its small enthalpy variation, may not be observed experimentally. In this framework, the two peaks observed in the thermal scans on samples S10 and S15 are so far in disagreement with results reported in [1].

3.2. Structural analysis

In order to assign the peaks evidenced by DSC to a given type of structural transformation, additional information is required and XRD tests were conducted at room temperature (RT-XRD).

X-ray diffraction profiles, shown in Fig. 2, reveal a multi-phase structure for all the three samples. Besides the peaks belonging to the austenite B2 structure, there are evidenced the reflections corresponding to the both type of martensite, namely orthorhombic (B19) and monoclinic (B19′) and to a cubic phase attributed to $Ti_2(NiCu)$. Starting from the above mentioned X-ray diffraction profiles, the relative phase content in the analyzed samples was estimated by Rietveld refinement (Fig. 3), obtained with the MAUD

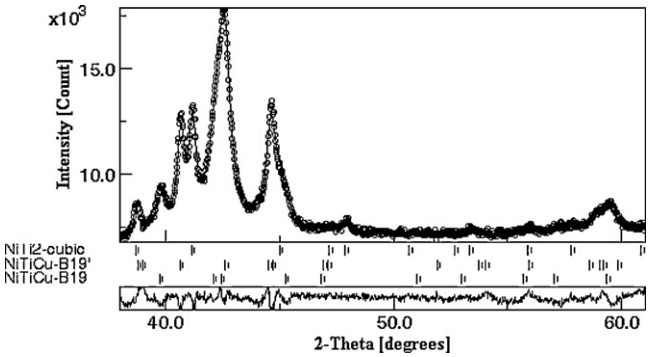

Fig. 3. Rietveld refinements for sample S15.

Table 1
Martensitic characteristic temperatures – Martensite start (Ms) and finish (Mf), austenite start (As) and finish, (Af) –, heat of transformation (ΔQ_{A-M} and ΔQ_{M-A}), range of martensitic transformation (Af–Mf) and thermal hysteresis (Af–Ms).

NiTiCu specimen	Ms [K]	Mf [K]	ΔQ_{A-M} [J/g]	As [K]	Af [K]	Af–Ms [K]	Af–Mf [K]	ΔQ_{M-A} [J/g]
S10	345	307	11.6	321	355	10	48	-10.0
S15	346	307	12.3	321	354	8	47	-10.71
S20	328	311	6.571	325	340	12.	29	-6.426

Table 2
Reliability parameters of the fit (GOF, Rp, Rwp) the phase's percentage for the sample obtained by mechanical milling taken from Rietveld refinements.

Sample	Parameters of fit	Percentage of phases			
		Monoclinic B19′ SG 11	Orthorhombic B19 SG 51	Ti2(NiCu) SG 227	Ti(NiCu) SG 221
S10	GOF = 2.36 Rp = 1.88% Rwp = 2.47%	27 ± 3	59 ± 4	11 ± 2	3 ± 0.5
S15	GOF = 1.95 Rp = 1.64% Rwp = 2.13%	41 ± 3	43 ± 3	15 ± 2	1 ± 0.5
S20	GOF = 1.98 Rp = 1.54% Rwp = 2.05%	60 ± 4	16 ± 2	21 ± 3	3 ± 1

software [9]. Table 2 presents the reliability parameters of the fit and the phase's percentage for the samples obtained at different milling times. After 10 h mechanical milling, the orthorhombic phase is the majority one and by increasing the milling time, the content of monoclinic and non-transforming $Ti_2(NiCu)$ phases increases. This last phase was generally reported in Ti rich NiTi based alloys prepared by classical routes but also in thin films or melt spun ribbons, being always induced after a thermal treatment [10,11]. For under discussion samples, the Ti_2Ni phase is most probably formed by a eutectic reaction at 942C during the sintering process (at 950C). Hence, the sintering process, performed identically on all samples, should not lead to the formation of a different amount of non-transforming phase, unless a different initial activation would be induced by the milling process. A longer time of milling causes evidently a higher amount of structural and compositional defects which seems to be related to the increasing content of the non-transforming phase. It is worth to mention at this point that according to Bertheville [12] the solid solubility of oxygen in NiTi is very small and when oxygen overpasses this level it stabilizes mainly the $Ti_4Ni_2O_x$ oxides. The oxide has the same f.c.c. structure like Ti_2Ni and the two compounds are not discernable by X-ray diffraction. So, the non-transforming phase observed by XRD could be equally attributed to Ti_2Ni but also to $Ti_4Ni_2O_x$ which expectedly has to be formed by dissolving the oxygen in the metallic matrix during the sintering process, especially in longer milled powders with a high amount of defects.

In order to prove the effect of milling on microstructure of the sintered samples, TEM observations were carried out. Besides a uniform dispersion of precipitates with sizes of 10–40 nm exhibited by the both investigated samples, a higher density of dislocations are evidenced on sample S20 comparatively to S10 (Fig. 4). Sample S20 presents also a higher density of nanotwin bands (noted by NT in Fig. 4b)

3.3. Discussion

The phases composition of the mechanical milled samples, as obtained by Rietveld refinement, can be finally correlated to the DSC results. The peak at higher temperature, which decreases and even disappears by increasing the milling time, may be attributed to the B2–B19 transformation in accord with the reduction content of orthorhombic phase revealed by the Rietveld refinement but also with the expected behavior for alloys with 20% at Cu. It is worth to mention that the above reasoning considers implicitly that the B2–B19 transformation is relatively enhanced for a relative higher amount of B19 phase in the sample at room temperature (where the X-ray diffraction data were obtained). Concerning the second transformation some consideration may be done. It is worth to notice that, for the alloy with the same composition prepared by powder metallurgy, it was reported a two step transformation [13] or a broad peak [8] in the DSC result; the transformation was ascribed to B2–B19–B19′ sequence, although the RT-XRD patterns evidenced peaks belonging to the both type of martensite, B19 and B19′. This pronounced increase of the temperature at which B19–B19′ transformation take place, in sample prepared by powder metallurgy, was attributed to the strain energy induced during milling; as effect of strain, the stability of the B19 martensite is decreased and the B19–B19′ transformation is induced [8]. However Goryczka and Van Humbeeck [7] evidenced, by temperature dependent X-ray diffractions, the transformation B2–B19 in TiNi30Cu20 alloy prepared by powder metallurgy after an adequate thermal treatment. It is to note that, the milling conditions are not clearly reported. However "rotating mixer" may suppose a low energy milling but

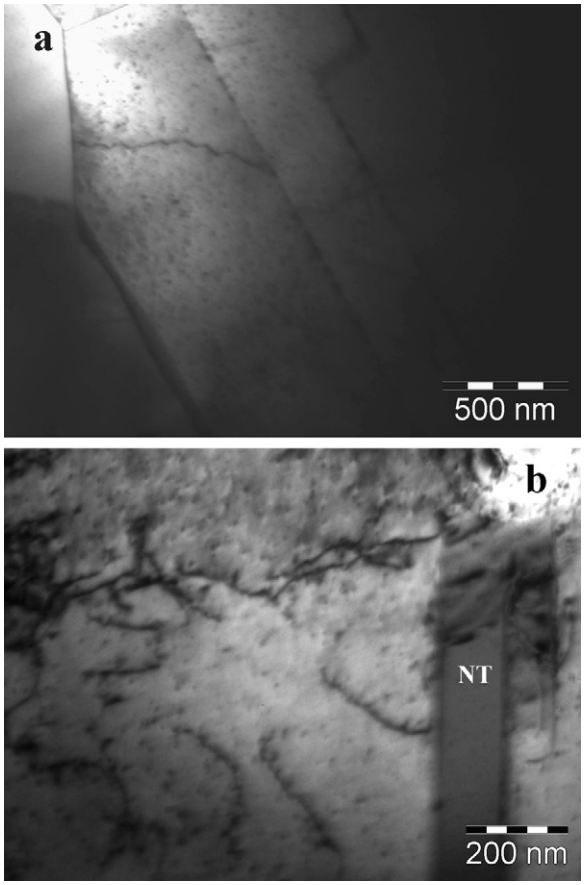

Fig. 4. TEM observation results on samples S10 and S20.

even in this conditions, the DSC peak is much larger (~40 K) compared with those observed in the alloy obtained by casting method (~8 K) [3] suggesting a different behavior in the alloys prepared by PM.

Returning to the second transformation in samples S10 and S15, although the X-ray diffraction patterns contain reflections corresponding to the monoclinic B19′ structure, recalling at a first view a two step transformation of type B2–B19–B19′, there are strong reasons to refute such behavior. If the second transition would be B19–B19′, then the majority phase at room temperature, should be of monoclinic structure (B19′), result which is not supported by the Rietveld refinement, especially for shorter time milled samples. Therefore, in accord with RT–XRD, the second transformation evidenced on these two samples, has to be assigned to B2–B19′. A supplemental reason for this assignment is given by the enthalpy of transformation. In DSC measurements, the peak area, representing the heat of transformation, is given by the chemical enthalpy variation (latent heat) as the main contribution, to which are added secondary terms for the stored elastic strain energy and the dissipated energy due to the interfacial friction. Accurate experimental investigations and thermodynamic calculations on Ti50Ni50–*x*Cu*x* alloy [14] show the following relation between the chemical enthalpies for the transformations under discussion: $\Delta H_{B2\rightarrow B19'} > \Delta H_{B2\rightarrow B19} > \Delta H_{B19\rightarrow B19'}$. In this context, the larger area of the second peak may be attributed to a transformation with larger enthalpy variation like B2–B19′ rather than to B19–B19′.

For the sample S20, the only one transformation evidenced by DSC had to be B2–B19′ in concordance with the high content of monoclinic structure given from Rietveld refinement and with its thermal location (similar to those observed in S10 and S15). However, the heat of transformation is less than that observed in the other samples for which the content of monoclinic structure was lower. Moreover, although X–ray diffraction evidenced also the orthorhombic phase of 16% relative content, the DSC did not evidenced the B2–B19 transformation. This may be due to the prolonged milling process with high rotating speed which damages the microstructure, induces dislocations, nanotwin bands (Fig. 4) and strains, increasing the probability of oxygen or carbon contamination; all these processes may alter the lattice elastic properties and change the transformation sequence. Hence, for a strained austenite structure, the transformation to an orthorhombic structure seems to be not energetically advantageously.

4. Conclusions

Starting from elemental powders, Ti50Ni30Cu20 shape memory alloys have been elaborated by mechanical milling for 10, 15 and 20 h. The crystalline structure and the characteristics of the martensitic transformation were investigated on samples obtained form powders after sintering and aging treatments. All the samples present martensitic transformation demonstrating the shape memory effect above room temperature with the transformation range (Af–Mf) of less than 50°.

By corroborating the X-ray diffraction data and the DSC results with thermodynamic considerations it was concluded that the martensitic transformation sequence B2–B19–B19′ observed in Ti50Ni30Cu20 alloys prepared by melting route is no more valid for the alloys prepared by mixing powders in high-energy mills. Instead, a two independent martensitic transformations namely B2–B19 and B2–B19′ take place. A longer milling process promote the formation of a non-transforming phase, $Ti_2(NiCu)$, and also reduces the heat of both type of transformations so that B2–B19 is not more evidenced by DSC.

Better results, concerning a good value for the heat of transformation, a narrow thermal hysteresis and a small quantity of impurity phase may be obtained from powders after a shorter mechanical milling process.

In Ti50Ni30Cu20 shape memory alloy prepared by powder metallurgy the martensitic transformation sequence is different than that evidenced in the alloy prepared by melting route. After a longer mechanical milling process the cubic (B2) to orthorhombic (B19) transformation is not more evidenced.

Acknowledgement

This work has been carried out with the financial support of the Romanian Ministry of Education (Projects PN09-450103 and PN71-116/2007).

References

[1] T.H. Nam, T. Saburi, Y. Nakata, K. Shimizu, Mater. Trans. JIM 31 (1990) 1050.
[2] T.H. Nam, T. Saburi, K. Shimizu, Mater. Trans. JIM 31 (1990) 959.
[3] H. Miyamoto, T. Taniwaki, T.K. Otsuka, S. Nishigori, K. Kato, Scripta Mater. 53 (2005) 171.
[4] T.H. Nam, S.G. Hur, I.S. Ahn, Met. Mater. 4 (1998) 61.
[5] Y. Liu, Mater. Sci. Eng. A354 (2003) 286.
[6] A. Terayama, H. Kyogoku, Mater. Sci. Eng. A 527 (2010) 5484.
[7] T. Goryczka, J. Van Humbeeck, J. Alloys Compd. 456 (2008) 194.
[8] S.H. Kang, S.G. Hur, H.W. Lee, T.H. Nam, Met. Mater. 6 (2000) 381.
[9] L. Lutterotti, P. Scardi, P. Maistrelli, J. Appl. Crystallogr. 25 (3) (1992) 459.
[10] A. Ishida, K. Ogawa, M. Sato, S. Miyazaki, Metall. Mater. Trans. A 28 (1997) 1985.
[11] T.H. Nam, C.A. Yu, Y.M. Nam, H.G. Kim, Y.W. Kim, J. Nanosci. Nanotechnol. 8 (2008) 722.
[12] B. Bertheville, J.E. Bidaux, J. Alloys Compd. 387 (2005) 211.
[13] A. Terayama, H. Kyogoku, J. Solid Mech. Mater. Eng. 3 (2009) 1057.
[14] W Tang, R. Sandstrom, Z.G. Wei, S. Miyazaki, Metall. Mater. Trans. A 31 (2000) 2423.